DOI: 10.1002/cplu.201300247

Mixed Co–Mn Oxide-Catalysed Selective Aerobic Oxidation of Vanillyl Alcohol to Vanillin in Base-Free Conditions

Ajay Jha,[a] Kashinath R. Patil,[b] and Chandrashekhar V. Rode*[a]

Manganese-doped cobalt mixed oxide (MnCo-MO) catalyst was prepared by a solvothermal method. The as-prepared catalyst was characterised by X-ray photoelectron spectroscopy, H_2 temperature-programmed reduction, O_2 temperature-programmed oxidation and XRD. This catalyst gave 62% conversion with 83% selectivity to vanillin in 2 hours for the liquid-phase air oxidation of vanillyl alcohol without using base. Three different types of metal oxides were observed in the prepared catalyst, which could be identified as Co_3O_4, Mn_3O_4 and $CoMn_2O_4$. Among these, the tetragonal phase of $CoMn_2O_4$ was found to be more active and selective for vanillyl alcohol oxidation than Co_3O_4 and Mn_3O_4. High-resolution TEM characterisation revealed the morphology of MnCo-MO nanorods with a particle size of 10 nm. Successful recycling of the catalyst was also established in this oxidation reaction.

Introduction

Mixed metal oxides play a very important role in academic as well as industrial research because of their acid–base and redox properties, and constitute the largest family of catalysts in heterogeneous catalysis.[1] Mixed metal oxides with a structure of spinel can be obtained by the substitution of metal cations from the host spinel oxide with other similar metal cations (dopants). This substitution may restructure chemical bonding at the surface of the host oxides, which modifies the electronic properties as well as the chemistry of the host metal oxides.[2] For example, doping of manganese into Co_3O_4 spinel leads to an increase in catalytic activity compared with the material that contains only a single metal, either cobalt or manganese, as an active phase.[3,4] The higher activity of the mixed metal oxides may be a cooperative effect towards an increment in the mobility of the oxygen as well as stabilising the more active species and favouring the redox cycles, which also permit the reactivation of the catalyst.[5] Zhang et al. used MnO_x-doped Co_3O_4 for the oxidation of CO in an H_2 stream. They proposed that the incorporation of MnO_x into Co_3O_4 increased the amounts of reactive oxygen species and adsorbed CO species over catalyst surfaces and enhanced the regeneration ability of the reduced catalyst by O_2.[6] Similarly, bimetallic copper–manganese oxide was reported for the liquid-phase aerobic oxidation of *p*-cresol to *p*-hydroxybenzaldehyde. It showed an excellent performance with 99% conversion and 96% selectivity to *p*-hydroxybenzaldehyde.[7] Another bimetallic combination of copper with cobalt (CoCu/C) has been used for the oxidation of *o*-cresol to salicylaldehyde.[8] The catalytic properties of Mn-doped Co_3O_4 catalyst are attributed to the ability of manganese to form oxides of different stoichiometries or mixed-valence compounds and their high oxygen storage capacity.[9] These metals (Co and Mn) are commonly used for oxidation reactions and also are more economical than noble-metal-based catalysts. Despite the large number of studies on single-component manganese[10–12] and cobalt oxides[13–16] and very few on mixed cobalt and manganese oxides for oxidation of volatile organic compounds (e.g., benzene and toluene), there is no single report addressing the catalytic properties based on the structural attributes of combinations of these two oxides for the aerobic oxidation of vanillyl alcohol, which is an industrially important phenolic starting compound.

The oxidation product of vanillyl alcohol is vanillin, which has a wide range applications in food and perfumes because of its flavour and also finds use in medicinal applications or as a platform chemical for pharmaceuticals production.[17–19] A great deal of work has been done on the synthesis of vanillin from guaiacol through the 1) nitrose and 2) glyoxalic acid methods.[17,20] However, these processes are known to give lower product yields (57%) associated with some serious drawbacks, such as formation of undesirable side products (nitrile and *p*-aminodimethylaniline) in the case of the nitrose method and use of toxic oxidants (CuO, PbO_2 and MnO_2)[21–23] in the glyoxalic acid method. Recently, Hu et al. reported the synthesis of vanillin from oxidation of 4-methylguaiacol by using [Co(salen)(py)][PF_6]$_2$ (salen = bis(salicylidene)ethylenediamine, py = pyridine) as the catalyst, to afford complete conversion with 86% selectivity to vanillin in 18 h with mediation of the reaction by NaOH.[24] Thereafter, a combination of cobaltous chlo-

[a] A. Jha, Dr. C. V. Rode
Chemical Engineering and Process Development
National Chemical Laboratory
Pune 411008 (India)
Fax: (+91) 20-2590-2621
E-mail: c.v.rode@ncl.res.in

[b] Dr. K. R. Patil
Centre for Materials Characterizations
NCL, Pune 411008 (India)

Supporting information for this article is available on the WWW under http://dx.doi.org/10.1002/cplu.201300247.

ride and *N*-hydroxyphthalimide-catalysed oxidation in the presence of NaOH was also reported for vanillin synthesis with complete conversion of 4-methylguaiacol and 90% product yield (vanillin) in 7 hours.[25] However, catalyst preparation in both the processes was complicated, requiring a long reaction time, and suffered a major problem in its recovery and recyclability. Hence, it is of great practical importance to develop a simplified preparation protocol for low-cost, highly active and reusable heterogeneous catalysts with the capability to form a strong redox couple and give controlled oxidation products.

Recently, we have been focussing on the development of efficient heterogeneous catalysts for liquid-phase oxidations of phenol derivatives.[26,27] This also includes use of Co_3O_4 nanoparticles for vanillyl alcohol oxidation in the presence of sodium hydroxide to give 80% conversion with 98% selectivity to vanillin in 6 hours.[27] In this oxidation, use of an excess amount of sodium hydroxide is mandatory for two reasons: firstly, it reacts with the phenolic –OH and prevents oxidation on the benzene ring; secondly, it prevents the formation of dimeric by-products and hence is beneficial for selective oxidation.[28] Nevertheless, the use of a large excess of sodium hydroxide has two major drawbacks: 1) catalyst deactivation owing to the formation of an inactive hydroxyl-bridged cobalt complex in the presence of water, and 2) formation of huge amounts of waste inorganic salt during product neutralisation. Hence, there is a genuine need to develop an oxidation route catalysed without using base. This would require a multifunctional solid catalyst designed in such a way that different active sites are present in the same catalyst for performing more than one function. Hence, we developed a manganese-doped cobalt mixed oxide (MnCo-MO) catalyst, synthesised by a solvothermal method, which showed an excellent activity for liquid-phase air oxidation of vanillyl alcohol to vanillin without using base (Scheme 1).

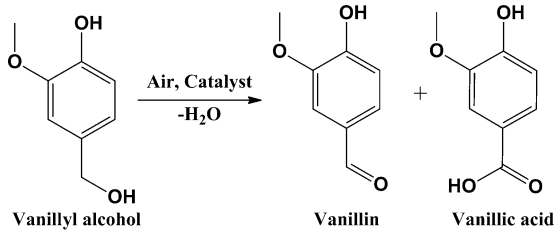

Scheme 1. Aerobic oxidation of vanillyl alcohol.

Results and Discussion

The XRD pattern of MnCo-MO catalyst in Figure 1 A shows diffraction peaks at $2\theta = 33.4$ (103), 39.1 (004) and 54.6° (312) corresponding to the tetragonal phase of $CoMn_2O_4$. The peaks at $2\theta = 24.7$ (101) and 41.5° (103) were attributed to the tetragonal phase of Mn_3O_4 and those at $2\theta = 19$, 31.4, 36.9, 44.9, 59.5 and 65.4° were ascribed to the cubic phase of Co_3O_4. Thus, the catalyst contained three different spinel oxides, namely $CoMn_2O_4$, Mn_3O_4 and Co_3O_4. Figure 1 B shows XRD profiles of both single and mixed metal oxides. Single-component cobalt

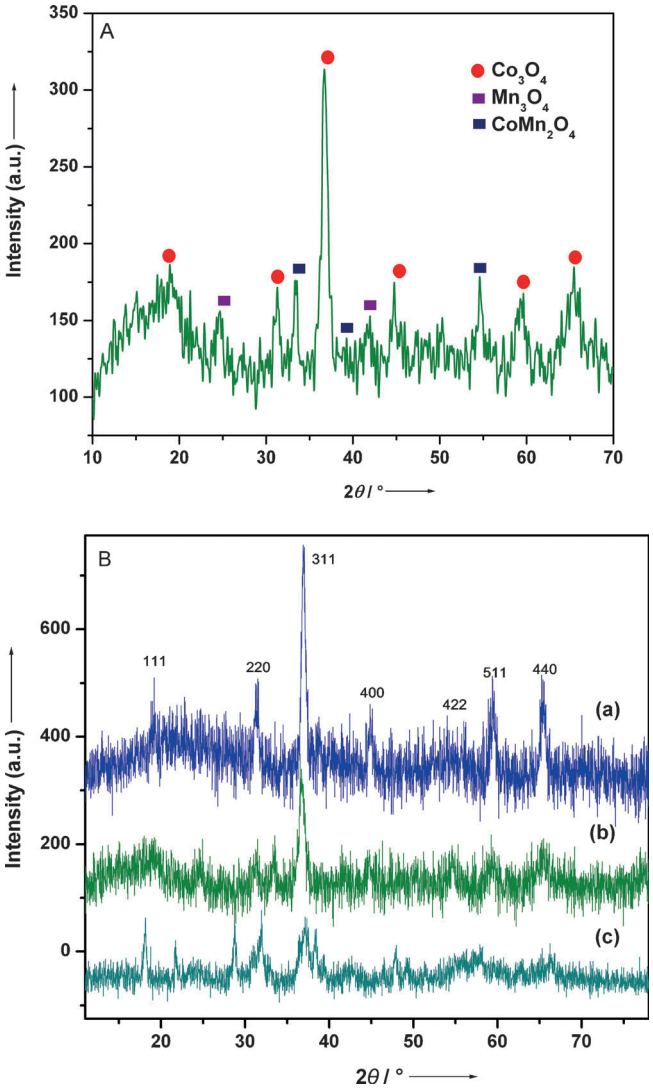

Figure 1. XRD patterns of A) MnCo-MO and B) Co_3O_4 (a), mixed oxide (b) and Mn_3O_4 (c).

and manganese samples on calcination showed diffraction phases that were related to Co_3O_4 and Mn_3O_4, respectively. The cobalt sample exhibited peaks at $2\theta = 19$ (111), 31.4 (220), 36.9 (311), 44.9 (400), 59.5 (511) and 65.4° (440), ascribed to the cubic phase of Co_3O_4 according to JCPDS No. 74-1657. The manganese sample exhibited a broad peak at $2\theta = 37°$ corresponding to the (112) plane of Mn_3O_4. The other peaks of lower intensity were also identical and matched those of the tetragonal hausmannite phase (JCPDS card No. 08-0017). In the case of MnCo-MO catalyst, the diffraction peaks of Co_3O_4 became weaker and broader after doping of manganese. The intensities of broad and small peaks in the XRD patterns of mixed oxides indicated that manganese caused some deformation in the crystal structure of Co_3O_4 that resulted in a decrease of particle size[29] (the crystallite size of Co_3O_4 was 14 nm, whereas it was 10 nm for MnCo-MO catalyst as calculated by using the Scherrer equation). Doping of manganese into the Co_3O_4 resulted in a slight shift in position from $2\theta = 36.9°$ towards a lower diffraction angle of $2\theta = 36.7°$ (311), which

might result from the insertion of manganese oxide in the octahedral framework of Co_3O_4.[30,31]

X-ray photoelectron spectroscopy (XPS) was used to monitor the oxidation states and the relative percentages of different constituent elements in the MnCo-MO catalyst and the results are shown in Table 1. A broad signal of Co $2p_{3/2}$ could be fitted satisfactorily to three principal peaks and one satellite peak after deconvolution, as shown in Figure 2a. The peak at 779.2 eV was assigned to the Co^{3+} of Co_2O_3 whereas the peak at 780 eV was assigned to the Co^{2+} of $CoMn_2O_4$.[32] Formation of $CoMn_2O_4$ was also confirmed by XRD and high-resolution transmission electron microscopy (HRTEM) results. $CoMn_2O_4$ is an incomplete normal spinel with a tetragonal structure in which Co^{2+} mainly occupies the tetrahedral sites and Mn^{3+} mainly occupies the octahedral sites. Another peak at 780.9 eV was also present owing to Co^{2+}, but from spinel Co_3O_4. A satellite peak at 782.8 eV was indicative of Co^{2+} in both the spinel Co_3O_4 and $CoMn_2O_4$. In the case of undoped Co_3O_4, the Co $2p_{3/2}$ peak could be deconvoluted into two major peaks, one at 780.2 eV (Co^{3+}) and the other at 782 eV (Co^{2+}); the very low intensity peak at 784 eV resulted from the 3d→4s shake-up satellite (Figure 2b), which was a characteristic of Co_3O_4.[33] We observed that doping of manganese into Co_3O_4 led to a decrease in the binding energy of cobalt species, which might be a result of formation of a Co–Mn compound ($CoMn_2O_4$), and it also reversed the Co^{2+}/Co^{3+} ratio in a mixed oxide relative to that in undoped cobalt oxide (Table 1).

Table 1. Surface composition calculated from XPS.

Catalyst	Atomic ratio (Co/Mn)	$CoMn_2O_4$	Co_3O_4		At.%[a]	
		Co^{2+} [%]	Co^{2+} [%]	Co^{3+} [%]	Mn	Co
MnCo-MO	2.6	40	27	33	27	73
Co_3O_4	–	–	33	67	–	–

[a] At.% = Atomic percent of Mn and Co in mixed oxide (MnCo-MO).

The MnCo-MO catalyst also showed a broad signal of Mn $2p_{3/2}$, which could be fitted satisfactorily to three major peaks and a satellite peak after deconvolution, as shown in Figure 2c. The peaks at 640.4, 641.4 and 642.4 eV correspond to Mn^{2+}, Mn^{3+} and Mn^{4+}, respectively,[9,34,35] whereas the small

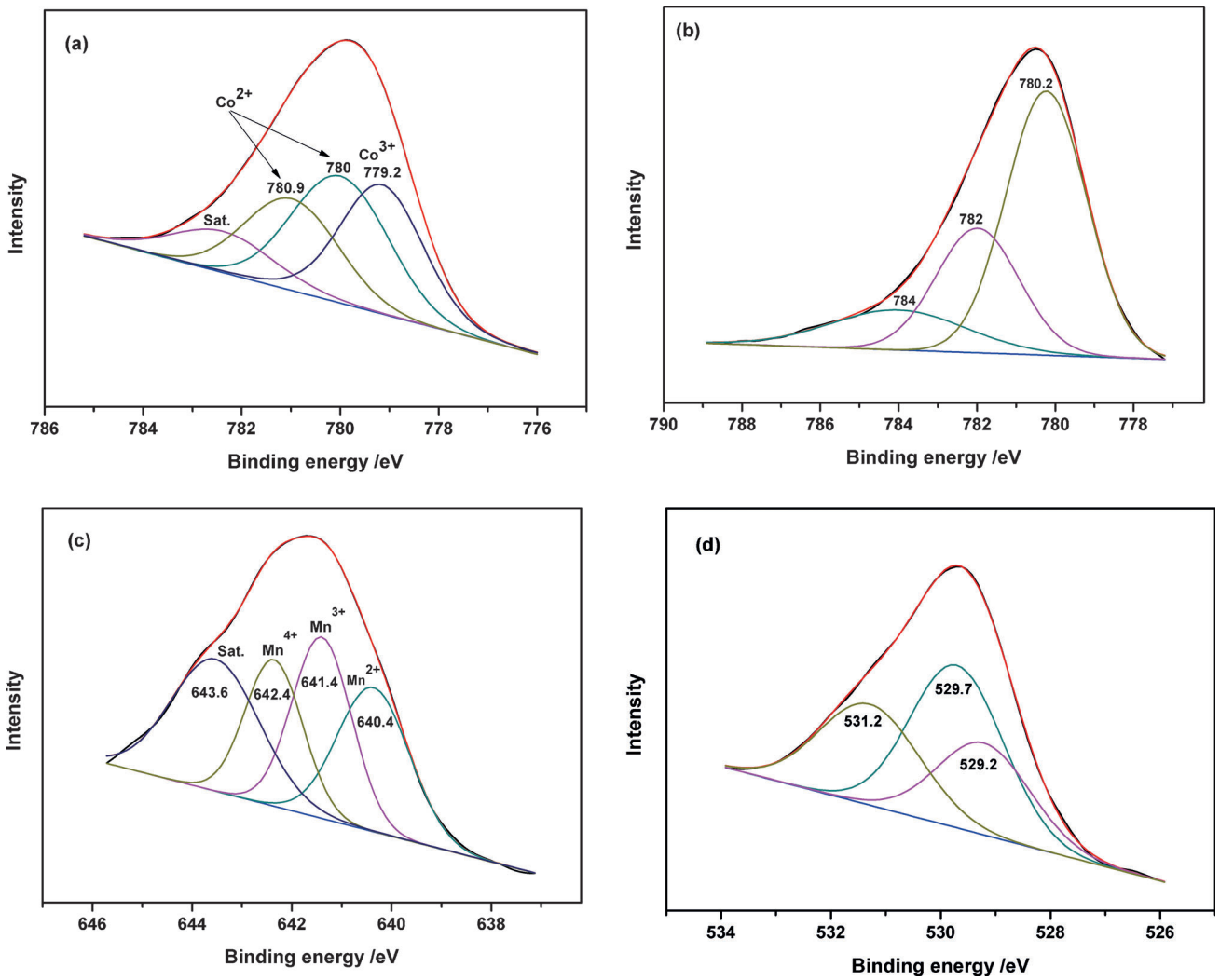

Figure 2. XPS of a) Co $2p_{3/2}$ of MnCo-MO, b) Co $2p_{3/2}$ of Co_3O_4, c) Mn $2p_{3/2}$ and d) O 1s of MnCo-MO catalyst.

peak at 643.6 eV corresponds to the satellite of Mn^{4+}. It is reasonable, therefore, to conclude that Mn element exists as Mn^{2+} and Mn^{3+} in both Mn_3O_4 and $CoMn_2O_4$ spinel oxides. The presence of these spinel oxides in MnCo-MO catalyst was also confirmed by XRD peaks at $2\theta = 24.7$ (101) and 33.4° (103), respectively. However, the presence of Mn^{4+} indicates the possibility of MnO_2, which we did not observe in XRD because of peak broadening.

The manner in which oxygen is bonded to metals in metal oxides can be determined through XPS of oxygen. In this series, the O 1s spectrum was used to identify the types of metal oxides present in MnCo-MO catalyst. In the O 1s spectrum of MnCo-MO, three peaks were fitted satisfactorily after deconvolution, as shown in Figure 2 d. The peaks at lower binding energies of 529.2 and 529.7 eV could be assigned to the lattice oxygen and must therefore correspond to Co–O and Mn–O bonds, respectively.[25,36] However, the peak at the higher binding energy of 531.2 eV was assigned to the surface-adsorbed oxygen (O^{2-} or O^-) or hydroxyl group or oxygen vacancies.[37]

Figure 3 shows HRTEM images of MnCo-MO catalyst, synthesised by the solvothermal method and subsequent calcination at 450 °C. As can be seen in Figure 3 b, the calcined

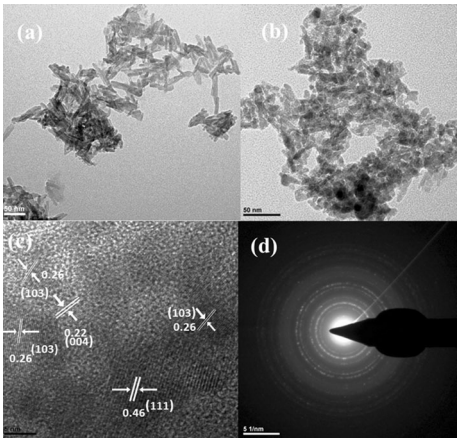

Figure 3. HRTEM images of MnCo-MO catalysts: a) as-synthesised catalyst; b) calcined sample. c) Lattice fringe patterns and d) SAED pattern.

sample displayed a roughly nanorod-like structure, whereas the as-synthesised sample showed a fully rod-like morphology with 79 nm length and 11 nm diameter (Figure 3 a). The average dimensions of calcined MnCo-MO nanorods were approximately 20–30 nm in length with a diameter of 4–7 nm. The lattice fringe patterns of the MnCo-MO catalyst are shown in Figure 3 c. The dominant exposed planes of MnCo-MO nanorods were (103) with a lattice spacing of 0.26 nm, which was related to the spinel $CoMn_2O_4$. The other exposed planes were (111) and (004) with a lattice spacing of 0.46 and 0.22 nm, related to the spinel Co_3O_4 and $CoMn_2O_4$, respectively. Figure 3 d shows the selected-area electron diffraction (SAED) pattern of the MnCo-MO catalyst, which was used to determine the lattice constants; the results were in excellent agreement with those obtained from XRD analysis.

To evaluate the reducibility and re-oxidisability as a function of the composition, both temperature-programmed reduction (TPR) and temperature-programmed oxidation (TPO) studies were performed for single and mixed metal oxides from 100 to 800 °C and the results are displayed in Figures 4 and 5, respectively. TPR of the manganese sample exhibited two peaks at

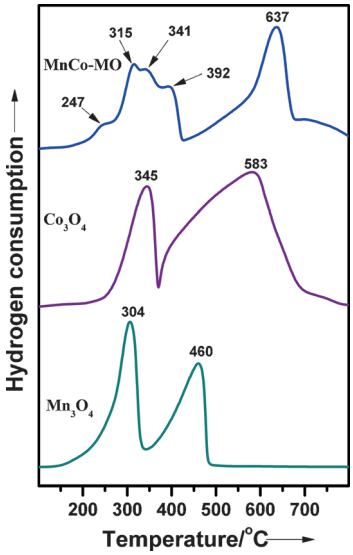

Figure 4. H_2-TPR profiles of Mn_3O_4, Co_3O_4 and MnCo-MO catalysts.

304 and 460 °C ascribed to the two-step reduction of MnO_2.[4,38] The H_2-TPR profile of Co_3O_4 was also characterised by two reduction peaks located at 345 and 583 °C (Figure 4), which resulted from a progressive reduction of Co_3O_4 as follows [Eq. (1)]:[39]

$$Co_3O_4 \rightarrow CoO \rightarrow Co^0 \quad (1)$$

The first reduction peak was very sharp and symmetrical with the temperature maximum centred at about 345 °C. This peak was associated with the reduction of trivalent cobalt oxide (Co_3O_4) to a divalent cobalt oxide (CoO) [Eq. (1)]. The second reduction peak was broad and unsymmetrical with a temperature maximum at about 583 °C, attributable to the subsequent reduction of divalent cobalt oxide (CoO) to metallic cobalt (Co^0).[40,41]

Four overlapping peaks at 247, 315, 341 and 392 °C were observed in the case of the manganese-doped cobalt oxide sample in a temperature range from 200 to 400 °C. It was noticed that the peak at 247 °C was observed only in the MnCo-MO sample, not for Co_3O_4 and Mn_3O_4 samples. It is reasonable to deduce that the peak at 247 °C resulted from the reduction of surface oxygen species generated by the presence of oxygen vacancies in MnCo-MO oxides. A similar observation was also reported by Shi et al. for $Mn_xCo_{3-x}O_4$ oxide used for formaldehyde oxidation.[42] The hydrogen consumption in a lower temperature range of 200–400 °C could be a result of the stepwise reduction of Co^{3+} to Co^{2+} and also of Mn^{4+} to Mn^{3+}. However, the peak in a higher temperature range of

400–700 °C could result from the reduction of Co^{2+} to Co^0 and Mn^{3+} to Mn^{2+} in a MnCo-MO sample.[43] The presence of the reduction peak at a higher temperature of approximately 637 °C in the TPR profiles of MnCo-MO catalysts (Figure 4) is additional evidence of the formation of mixed Co–Mn oxides.[4]

After reduction of single (Co_3O_4 and Mn_3O_4) and mixed metal oxides (MnCo-MO) to the corresponding metallic forms during TPR experiments, TPO experiments were also performed and the results are displayed in Figure 5. The addition

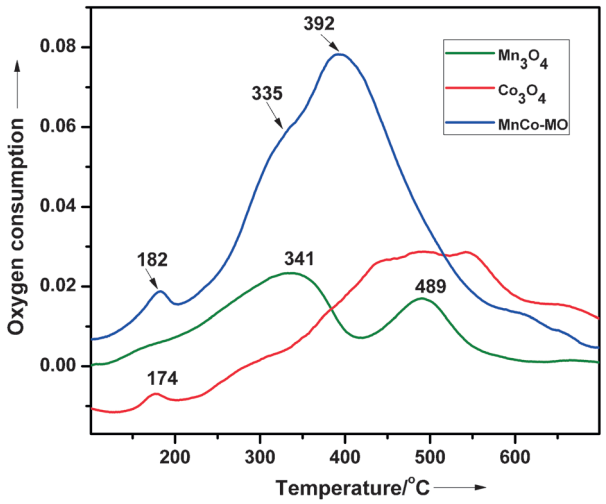

Figure 5. O_2-TPO profiles of Mn_3O_4, Co_3O_4 and MnCo-MO catalysts.

of manganese to cobalt oxide led to remarkable changes in the TPO profiles of single metal oxides with respect to the amount of oxygen consumed, number of oxidation peaks and the oxidation temperature. If the reduced MnCo-MO catalyst was exposed to oxygen, manganese was oxidised to a great extent and the resulting manganese oxide covered the cobalt oxide peaks. So we could not distinguish the separate oxidation peaks for Mn and Co oxides. As can be seen from Figure 5, the area of the oxygen consumption peak for MnCo-MO catalyst was higher than that of the oxygen consumption peak for single metal oxides. This observation indicates that the addition of manganese to cobalt oxide enhanced the consumption of oxygen in mixed metal oxides.

Catalytic activity

The activity of single metal oxides (Co_3O_4 and Mn_3O_4) was compared with that of mixed metal oxide (MnCo-MO) catalysts for the liquid-phase air oxidation of vanillyl alcohol and the results are shown in Figure 6. Among these catalysts, Co_3O_4 showed significantly lower substrate conversion (48%) with higher selectivity to vanillin (88%). The efficiency of Mn_3O_4 in terms of vanillin yield was marginally higher (54%) than that obtained for MnCo-MO catalyst (51%), but the catalyst recycling experiment with Mn_3O_4 showed a substantially diminished conversion of 29% and also lower selectivity to vanillin (74%) owing to the higher oxygen storage capacity and faster oxygen absorption rates of manganese oxide (MnO_x), which led to the

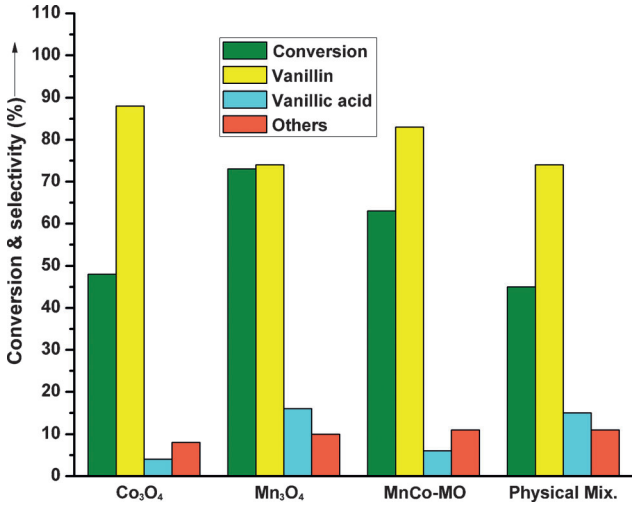

Figure 6. Catalyst screening for oxidation of vanillyl alcohol. Reaction conditions: vanillyl alcohol (3.24 mmol), catalyst (0.1 g), 140 °C, acetonitrile (70 mL), air pressure (21 bar), time 2 h.

over-oxidation to vanillic acid. However, the MnCo-MO catalyst showed superior recyclability (discussed later) and selectivity to vanillin of 83% relative to catalysts containing only the single oxide of either cobalt or manganese. The higher activity of the MnCo-MO catalyst might result from spinel $CoMn_2O_4$ along with Mn species of varying oxidation states. A separate oxidation experiment performed by using a physical mixture of Mn_3O_4 and Co_3O_4 showed only 45% conversion of vanillyl alcohol with 74% selectivity to vanillin, which was close to that obtained for spinel Co_3O_4. The importance of Co/Mn composition in the mixed metal oxide was also studied by preparing and testing two mixed oxide samples with varying molar ratios of Mn and Co (MnCo 1:1 and 2:1). Both of these catalysts showed either inferior activity and/or selectivity relative to MnCo-MO catalyst with 1:2 molar ratio of Mn and Co. MnCo 1:1 catalyst showed 52% conversion and 83% selectivity to vanillin, whereas MnCo 2:1 showed 64% conversion of vanillyl alcohol with 74% selectivity to vanillin (Table S1 in the Supporting Information). The lower selectivity to vanillin in the case of MnCo 2:1 catalyst was owing to the over-oxidation of vanillin to vanillic acid. MnCo-MO having a Mn/Co ratio of 1:2, prepared by a co-precipitation method,[44] on testing for vanillyl alcohol oxidation showed inferior activity (22% conversion) to MnCo-MO prepared by a solvothermal method (Table S1). In spite of the fact that MnCo-MO prepared by co-precipitation had a pure $CoMn_2O_4$ phase, it had a very low activity because of its lower surface area (17 $m^2 g^{-1}$) and higher crystallite size (62 nm) than MnCo-MO prepared by the solvothermal method, which had a higher surface area of 105 $m^2 g^{-1}$ and smaller crystallite size of 10 nm (Figure S1).

Further, the nature of the solvent was also found to have a profound influence on vanillyl alcohol oxidation. The sequential oxidation of aldehyde to acid and other by-products may be inhibited through careful selection of the solvent. In a nonpolar solvent such as toluene, poor conversion of vanillyl alcohol was obtained (35%) owing to the lower solubility of vanillyl alcohol in toluene. Among the polar solvents, organic polar

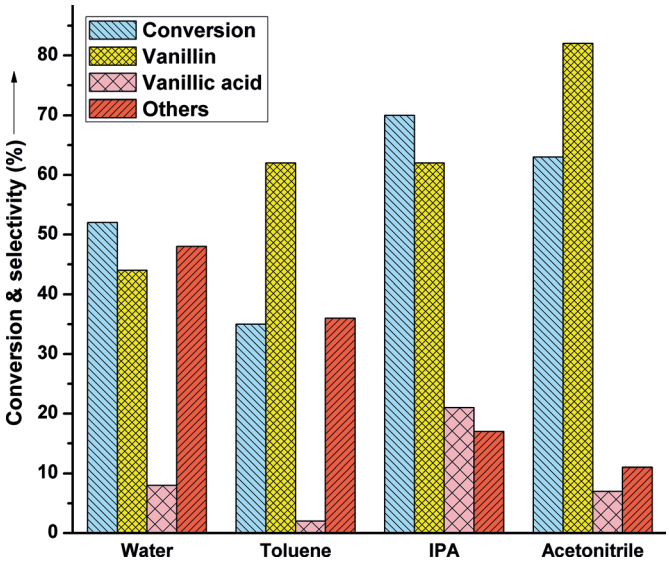

Figure 7. Effect of solvent on the oxidation of vanillyl alcohol. Reaction conditions: vanillyl alcohol (3.24 mmol), MnCo-MO catalyst (0.1 g), 140 °C, solvent (70 mL), air pressure (21 bar), time 2 h. IPA = isopropyl alcohol.

solvents showed a better performance than inorganic solvent (H_2O), which might be because of the higher solubility of oxygen in organic solvents. As can be seen from Figure 7, the conversion and selectivity were remarkably different in polar inorganic and polar organic solvents. In water, conversion of vanillyl alcohol was 52% and selectivity to vanillin was only 44% with majority formation of tar. Vanillyl alcohol is sparingly soluble in water; hence significant inhibition of the adsorption of the substrate onto the catalyst surface restricts the rate of reaction. However, in polar organic solvent, the solubility of the substrate was higher allowing easy adsorption of reactant molecules on the catalyst surface and the reaction was readily facilitated. Oxidation of vanillyl alcohol in acetonitrile gave the highest conversion of 62% and selectivity of 83% to vanillin compared with oxidation in isopropyl alcohol (60% conversion of vanillyl alcohol with 62% selectivity to vanillin). The higher dielectric constant of acetonitrile (37.5) than that of isopropyl alcohol (17.9) facilitates better solubility of substrate and oxidant in the solvent, hence affecting the activity and selectivity pattern.

The effect of reaction time on vanillyl alcohol conversion and selectivity to vanillin was studied with MnCo-MO catalyst under optimised reaction conditions and the results are shown in Figure 8. The conversion of vanillyl alcohol increased from 43 to 63% and the selectivity to vanillin increased from 79 to 83% with an increase in reaction time from 1 to 2 hours. A further increase in reaction time from 2 to 4 hours enhanced the conversion of vanillyl alcohol from 63 to 80%; however, it led mainly to the formation of tar. As this could not be detected by HPLC, the material balance of the overall reaction was <90%. The visible tarry product was separated out from the reaction crude, dried, weighed and accounted for determining the vanillin selectivity as well. The selectivity of vanillin was found to decrease from 83 to 72% with increase in reaction time from 2 to 4 hours.

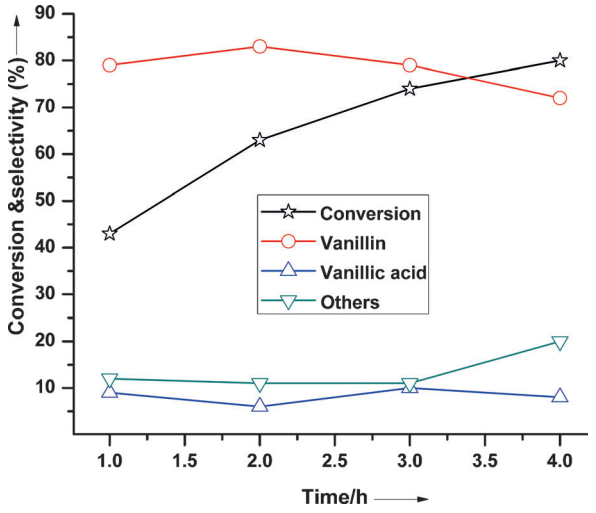

Figure 8. Effect of reaction time on vanillyl alcohol oxidation. Reaction conditions: vanillyl alcohol (3.24 mmol), MnCo-MO catalyst (0.1 g), 140 °C, acetonitrile (70 mL), air pressure (21 bar).

The effect of temperature on vanillyl alcohol oxidation was examined over the MnCo-MO catalyst in a temperature range of 100–160 °C and the results are shown in Figure 9. The conversion of vanillyl alcohol increased from 41 to 76% with an increase in reaction temperature from 100 to 160 °C. The selectivity to vanillin increased from 57 to 83% initially with an increase in reaction temperature from 100 to 140 °C, but a further increase in temperature to 160 °C caused a decrease in vanillin selectivity from 83 to 74% owing to the formation of over-oxidation products.

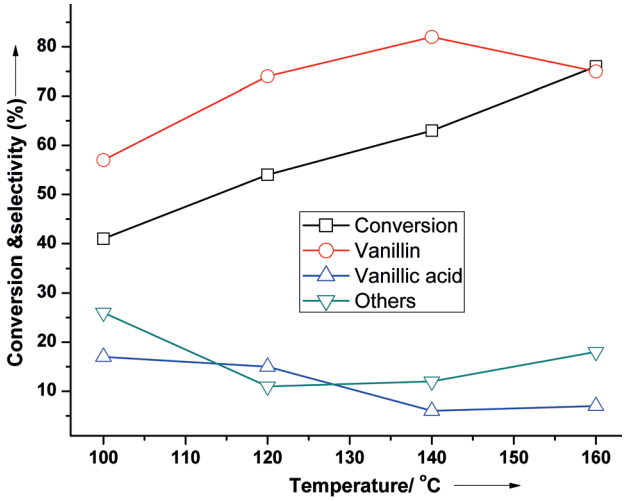

Figure 9. Effect of temperature on vanillyl alcohol oxidation. Reaction conditions: vanillyl alcohol (3.24 mmol), MnCo-MO catalyst (0.1 g), 100–160 °C, acetonitrile (70 mL), air pressure (21 bar), time 2 h.

Catalyst concentration has a significant effect on the liquid-phase oxidation of vanillyl alcohol. Experiments were conducted by varying the catalyst concentration in the range of 0.0007–0.0017 g cm^{-3} and the results are displayed in Figure 10. The conversion of vanillyl alcohol increased with in-

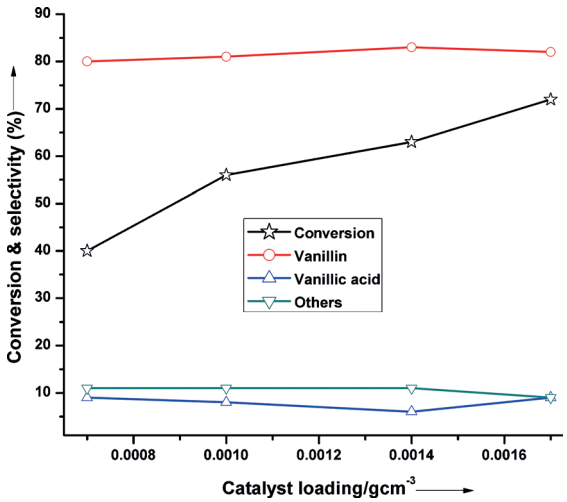

Figure 10. Effect of catalyst concentration on vanillyl alcohol oxidation. Reaction conditions: vanillyl alcohol (3.24 mmol), MnCo-MO catalyst (0.0007–0.0017 g cm^{-3}), 140 °C, acetonitrile (70 mL), air pressure (21 bar), time 2 h.

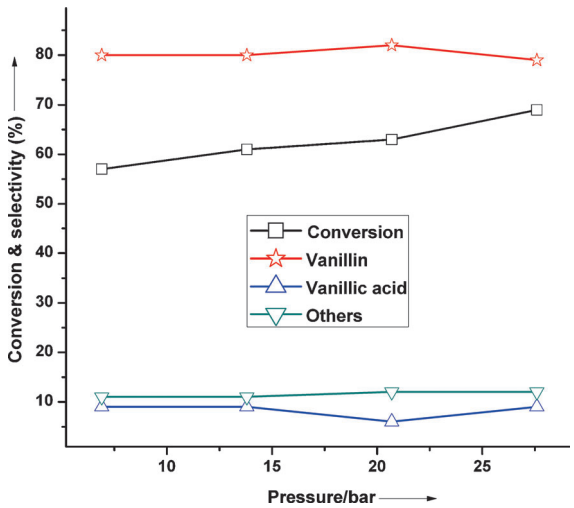

Figure 11. Effect of pressure on vanillyl alcohol oxidation. Reaction conditions: vanillyl alcohol (3.24 mmol), MnCo-MO catalyst (0.1 g), 140 °C, acetonitrile (70 mL), air pressure (7–28 bar), time 2 h.

crease in catalyst loading from 0.0007 to 0.0014 g cm^{-3}, whereas the selectivity to vanillin remained almost constant at about 83%. The increase in conversion with increase in catalyst loading was a result of the increase in the number of active sites available for participating in the reaction. Further increase in catalyst loading from 0.0014 to 0.0017 had a marginal effect on vanillyl alcohol conversion, thus implying that mass-transfer resistance could be significant under these conditions.

The effect of partial pressure of oxygen on conversion and selectivity was studied for vanillyl alcohol oxidation by varying the air pressure in the range of 7 to 28 bar at 140 °C and the results are shown in Figure 11. Both the conversion of vanillyl alcohol and selectivity to vanillin increased gradually with an increase in air pressure from 7 to 21 bar, beyond which the conversion increased but the selectivity to vanillin started decreasing from 83 to 78%, thereby implying that a higher dissolved concentration of oxygen increased the formation of other by-products.

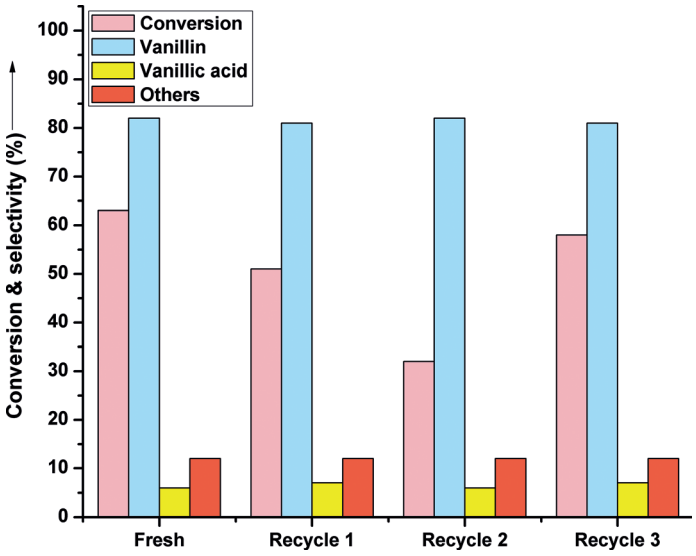

Figure 12. MnCo-MO catalyst recycling studies. Reaction conditions: vanillyl alcohol (3.24 mmol), MnCo-MO catalyst (0.1 g), 140 °C, acetonitrile (70 mL), air pressure (21 bar), time 2 h.

The stability of the MnCo-MO catalyst for vanillyl alcohol oxidation was investigated by recycling studies in the following way. After the first oxidation run with fresh MnCo-MO catalyst, the reaction crude was allowed to settle and the clear supernatant product mixture was removed from the reactor. The catalyst remaining in the reactor was washed with methanol twice and then dried at 100 °C. The subsequent run was continued by adding a fresh charge to this catalyst. Figure 12 shows that the activity decreased if only the dried reused catalyst was used (recycles 1 and 2), but the original activity could be regained (63%) if the reused catalyst (recycle 3) was calcined again at 450 °C for 1 hour. A small loss in the activity was observed, which resulted from handling of the catalyst.

To eliminate the possibility of a homogeneously catalysed reaction owing to dissolution of metal oxide, a leaching test was also performed as follows. The MnCo-MO catalyst was separated from the reaction mixture by simple filtration after a partial conversion of 43% in 1 hour, and the filtrate was then employed in further reaction under similar conditions (21 bar air pressure at 140 °C), which did not give any further conversion. The absence of any metal species in the filtrate was also confirmed by inductively coupled plasma spectrometry. These results clearly support the fact that the oxidation of vanillyl alcohol catalysed by MnCo-MO is truly heterogeneous in nature.

A plausible mechanistic pathway for oxidation of vanillyl alcohol catalysed by mixed oxide (MnCo-MO) to give vanillin is shown in Scheme 2. In the ground state, oxygen remains in the triplet form containing two unpaired electrons with parallel spins. Direct reaction of triplet oxygen with singlet organic

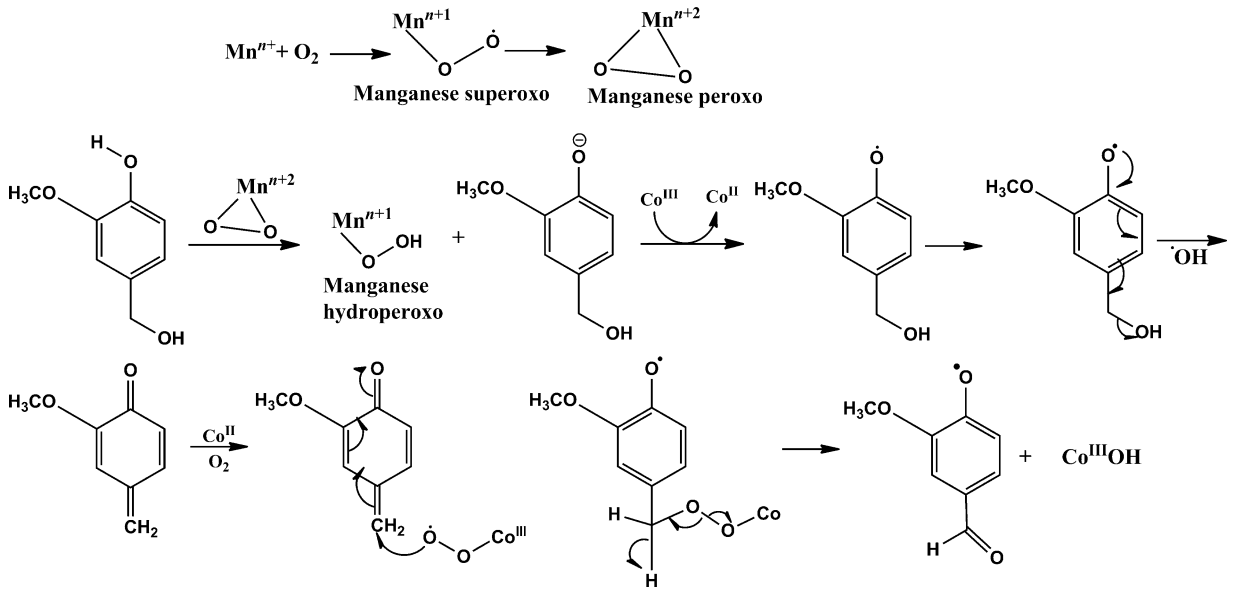

Scheme 2. Plausible mechanistic pathway for the formation of vanillin.

molecules to give a singlet product is a spin-forbidden process and has a very slow reaction rate. This can be overcome by complexation of triplet oxygen with a paramagnetic transition-metal ion.[45] As manganese with d^4 configuration has a more paramagnetic nature (2.8 BM) than cobalt with d^7 configuration (1.7 BM) in a tetragonal complex because of the Jahn–Teller effect,[46] it has a strong tendency to react with an oxygen molecule to give a metal superoxo complex. This then further converts into the metal peroxo complex, which readily forms a metal hydroperoxo complex by abstracting a proton from vanillyl alcohol to give the corresponding phenolate ions. The role of Mn is thus significant in eliminating the use of a free base (NaOH). The phenolate ions get oxidised to the phenoxy radical by means of reaction with Co^{III} species present in the reaction medium.[47] The phenoxy radical then undergoes further reaction to form the quinomethide, which reacts with the cobalt superoxo complex to give a peroxycobalt(III) complex followed by its subsequent decomposition to the corresponding aldehyde with concomitant release of a hydroxycobalt(III) complex. The formed aldehyde with a free radical abstracts the proton from the reaction medium and is converted to vanillin.

To examine the involvement of free radicals in the reaction, we performed the oxidation reaction in the presence of a small amount of radical scavenger, benzoquinone, under the same reaction conditions. The conversion of vanillyl alcohol dropped significantly from 62 to 25% without affecting the selectivity, thus supporting the role of free radicals in the reaction.

Conclusion

A mixed oxide (MnCo-MO) catalyst has been prepared by a solvothermal method and its catalytic activity was evaluated in the liquid-phase aerobic oxidation of vanillyl alcohol in the absence of base. Doping of manganese into the Co_3O_4 framework led to the formation of tetragonal $CoMn_2O_4$ and Mn_3O_4 spinel phases. The existence of $CoMn_2O_4$ was confirmed by XRD, HRTEM and XPS. TPR also gave additional evidence of the formation of mixed Co–Mn oxides by the appearance of a reduction peak at a higher temperature (≈637 °C). TPO of a mixed oxide exhibited higher oxygen adsorption capacity than that of a single metal oxide, which was the reason for the higher activity of the mixed oxide catalysts. The prepared material showed a rod-like morphology, as confirmed by HRTEM. Our catalyst could be successfully recycled three times and no metal leaching was observed.

Experimental Section

Catalyst preparation

Manganese-doped cobalt oxide catalyst was prepared by a solvothermal method keeping the molar ratio of Co/Mn = 2. In a typical synthesis, manganese acetate tetrahydrate (2.45 g) and cobalt acetate tetrahydrate (4.98 g) were dissolved in ethylene glycol (60 mL), the solution was heated gradually from room temperature to 160 °C, and then 0.3 M aqueous Na_2CO_3 solution (200 mL) was added dropwise. The resulting slurry was further aged for 1 h under a nitrogen atmosphere. The product was isolated by filtration, washed thoroughly with distilled water until neutralisation, dried at 100 °C for 12 h, then calcined at 450 °C for 4 h. The obtained catalyst was labelled MnCo-MO. Single-component Co_3O_4 and Mn_3O_4 catalysts were also prepared by the same method. In addition, MnCo-MO was prepared by a co-precipitation method as described earlier.[44]

Characterisation

X-ray diffractograms of the catalysts were recorded in the 2θ range of 10–80° (scan rate 5.3° min^{-1}) on a PANalytical PXRD Model X-Pert PRO-1712 instrument, with Ni-filtered CuK_α radiation (λ = 0.154 nm) as source (current intensity, 30 mA; voltage, 40 kV) and

an Xcelerator detector. Temperature-programmed reduction (TPR) experiments were performed on a Micromeritics Chemisorb 2720 instrument: the catalyst (0.02 g) was placed in a quartz tube and treated with argon gas (25 mL min^{-1}) at 200 °C for 1 h. A gas mixture of 5% hydrogen in argon was then passed through the quartz reactor at 50 °C for 1 h. The temperature was raised from room temperature to 900 °C at a heating rate of 10 K min^{-1} and held at 900 °C for 10 min. The reduced sample was then subjected to temperature-programmed oxidation (TPO). X-ray photoelectron spectroscopy (XPS) analysis was performed on a VG Scientific ESCA-3000 spectrometer by using non-monochromatised MgK_{α} radiation (1253.6 eV). To correct for possible deviations caused by electric charge of the samples, the C 1s line at 284.6 eV was taken as an internal standard.

Catalytic reaction

All the catalytic oxidation reactions were performed in a 300 cm^3 capacity high-pressure Hastelloy reactor supplied by Parr Instruments Co. USA. The reactor was connected to an air reservoir held at a pressure higher than that of the reactor. A Thermo Scientific model AS3000 liquid chromatograph equipped with an ultraviolet detector was used for the analysis. HPLC analysis was performed on a 25 cm RP-18 column. The product and reactant were detected with a UV detector at $\lambda_{max} = 254$ nm. Aqueous methanol (50%) was used as mobile phase at a column temperature of 35 °C and a flow rate of 0.7 mL min^{-1}.

In a typical experiment, vanillyl alcohol (0.5 g), catalyst (0.1 g) and acetonitrile (70 mL) were charged into a 300 mL Parr autoclave. The reaction mixture was heated to 140 °C. After the desired temperature was attained, the reactor was pressurised with 21 bar air pressure. Then the reaction was started by agitating at 1000 rpm. The reaction was continued for up to 2 h, then the reactor was cooled to room temperature and the unabsorbed air was vented out. The content of the reactor was discharged and the final volume was noted.

Acknowledgements

A.J. gratefully acknowledges the Council of Scientific and Industrial Research (CSIR, New Delhi) for the award of a senior research fellowship.

Keywords: aerobic oxidation · cobalt · heterogeneous catalysis · manganese · spinel phases

[1] M. B. Gawande, R. K. Pandey, R. V. Jayaram, *Catal. Sci. Technol.* **2012**, *2*, 1113 – 1125.
[2] E. W. McFarland, H. Metiu, *Chem. Rev.* **2013**, *113*, 4391 – 4427.
[3] Z. Tian, P. H. T. Ngamou, V. Vannier, K. Kohse-Hőinghaus, N. Bahlawane, *Appl. Catal. B* **2012**, *117 – 118*, 125 – 134.
[4] S. Todorova, H. Kolev, J. P. Holgado, G. Kadinov, Ch. Bonev, R. Pereñíguez, A. Caballero, *Appl. Catal. B* **2010**, *94*, 46 – 54.
[5] D. A. Aguilera, A. Perez, R. Molina, S. Moreno, *Appl. Catal. B* **2011**, *104*, 144 – 150.
[6] Q. Zhang, X. Liu, W. Fan, Y. Wang, *Appl. Catal. B* **2011**, *102*, 207 – 214.
[7] F. Wang, G. Yang, W. Zhang, W. Wu, J. Xu, *Adv. Synth. Catal.* **2004**, *346*, 633 – 638.
[8] F. Wang, J. Xu, S. Liao, *Chem. Commun.* **2002**, 626 – 627.
[9] S. Todorova, A. Naydenov, H. Kolev, J. P. Holgado, G. Ivanov, G. Kadinov, A. Caballero, *Appl. Catal. A* **2012**, *413 – 414*, 43 – 51.
[10] J. Trawczyński, B. Bielak, W. Miśta, *Appl. Catal. B* **2005**, *55*, 277 – 285.
[11] M. Baldi, E. Finocchio, F. Milella, G. Busca, *Appl. Catal. B* **1998**, *16*, 43 – 51.
[12] A. Gil, L. M. Gandía, S. A. Korili, *Appl. Catal. A* **2004**, *274*, 229 – 235.
[13] V. S. Kshirsagar, S. Vijayanand, H. S. Potdar, P. A. Joy, K. R. Patil, C. V. Rode, *Chem. Lett.* **2008**, *37*, 310 – 311.
[14] C. V. Rode, M. V. Sonar, J. M. Nadgeri, R. V. Chaudhari, *Org. Process Res. Dev.* **2004**, *8*, 873 – 878.
[15] A. C. Garade, N. S. Biradar, S. M. Joshi, V. S. Kshirsagar, R. K. Jha, C. V. Rode, *Appl. Clay Sci.* **2011**, *53*, 157 – 163.
[16] X. Xie, Y. Li, Z. Liu, M. Haruta, W. Shen, *Nature Lett.* **2009**, *458*, 746 – 749.
[17] S. R. Rao, G. A. Ravishankar, *J. Sci. Food Agric.* **2000**, *80*, 289 – 304.
[18] H. Priefert, J. Rabenborst, A. Steinbüchel, *Appl. Microbiol. Biotechnol.* **2001**, *56*, 296 – 314.
[19] A. Sheldrak, *Nature* **1972**, *238*, 352.
[20] A. D. Bulam, S. V. Nekrasov, B. V. Passet, V. G. Foshkin, *J. Appl. Chem. USSR.* **1988**, *61*, 859.
[21] Y. Chang, M. Zhang, L. Xia, J. Zhang, G. Xing, *Materials* **2012**, *5*, 2850 – 2871.
[22] N. J. Hill, J. M. Hoover, S. S. Stahl, *J. Chem. Educ.* **2013**, *90*, 102 – 105.
[23] J. KamLet, E. Conn, SU Pat. 2640083, **1953**.
[24] J. Hu, Y. Hu, J. Mao, J. Yao, Z. Chena, H. Li, *Green Chem.* **2012**, *14*, 2894 – 2898.
[25] Y. Zhang, X. Li, X. Cao, J. Zhao, *Res. Chem. Intermed*, **2013** DOI: 10.1007s11164 – 013 – 1039-x.
[26] M. Biswal, V. V. Dhas, V. R. Mate, A. Banerjee, P. Pachfule, K. L. Agrawal, S. B. Ogale, C. V. Rode, *J. Phys. Chem. C* **2011**, *115*, 15440 – 15448.
[27] A. Jha, C. V. Rode, *New J. Chem.* **2013**, *37*, 2669 – 2674.
[28] F. Wang, G. Yang, W. Zhang, W. Wu, J. Xu, *Chem. Commun.* **2003**, 1172 – 1173.
[29] J. Li, X. Liang, S. Xu, J. Hao, *Appl. Catal. B* **2009**, *90*, 307 – 312.
[30] F. Morales, D. Grandjean, A. Mens, F. M. F. de Groot, B. T. Weckhuysen, *J. Phys. Chem. B* **2006**, *110*, 8626 – 8639.
[31] Q. Liang, K. D. Chen, W. H. Hou, Q. J. Yan, *Appl. Catal. A* **1998**, *166*, 191 – 199.
[32] C. D. Wagner, J. F. Moulder, L. E. Davis, W. M. Riggs, *Handbook of X-ray Photoelectron Spectroscopy, 1st ed* (Ed.: G. E. Muilenberg), Perkin-Elmer Corporation, Physical Electronics Division, Eden Prairie, **1979**.
[33] B. Tan, K. J. Klabunde, P. M. A. Sherwood, *J. Am. Chem. Soc.* **1991**, *113*, 855 – 861.
[34] S. Ponce, M. A. Pena, J. L. G. Fierro, *Appl. Catal. B* **2000**, *24*, 193 – 205.
[35] D. Delimaris, T. Ioanides, *Appl. Catal. B* **2008**, *84*, 303 – 312.
[36] C. Liu, Q. Liu, L. Bai, A. Dong, G. Liu, S. Wen, *J. Mol. Catal. A* **2013**, *370*, 1 – 6.
[37] J. Li, S. Xiong, X. Lia, Y. Qian, *J. Mater. Chem.* **2012**, *22*, 23254 – 23259.
[38] M. Ferrandon, J. Carnö, S. Järås, E. Björnbom, *Appl. Catal. A* **1999**, *180*, 141 – 151.
[39] J. Luo, M. Meng, X. Li, *J. Catal.* **2008**, *254*, 310 – 324.
[40] P. Arnoldy, J. A. Moulijn, *J. Catal.* **1985**, *93*, 38 – 54.
[41] W. J. Xue, Y. F. Wang, P. Li, Z. Liu, Z. P. Hao, C. Y. Ma, *Catal. Commun.* **2011**, *12*, 1265 – 1268.
[42] C. Shi, Y. Wang, A. Zhu, B. Chen, C. Au, *Catal. Commun.* **2012**, *28*, 18 – 22.
[43] K. Jirátová, J. Mikulová, J. Klempa, T. Grygar, Z. Bastl, F. Kovanda, *Appl. Catal. A* **2009**, *361*, 106 – 116.
[44] S. A. Hosseini, D. Salari, A. Niaei, F. Deganello, G. Pantaleo, P. Hojati, *J. Environ. Sci. Health Part A* **2011**, *46*, 291 – 297.
[45] R. A. Sheldon, R. A. van Santen, *Catalytic Oxidation: Principles and Applications*, World Scientific, Singapore, **1995**, pp. 12 – 13.
[46] J. E. Huheey, E. A. Keiter, R. L. Keiter, O. K. Medhi, *Inorganic Chemistry: Principles of Structure and Reactivity*, Pearson Education, Upper Saddie River, NJ, **2008**, pp. 489.
[47] B. Barton, C. G. Logie, B. M. Schoonees, B. Zeelie, *Org. Process Res. Dev.* **2005**, *9*, 62 – 69.

Received: July 4, 2013
Revised: September 3, 2013
Published online on October 14, 2013